Proceedings of ASME Turbo Expo 2011
GT2011
June 6-10, 2011, Vancouver, British Columbia, Canada

GT2011-46078

EFFECTS OF PIN DETACHED SPACE ON HEAT TRANSFER IN A RIB ROUGHENED CHANNEL

Sin Chien Siw
Minking K. Chyu
Department of Mechanical Engineering and Materials Science
University of Pittsburgh
Pittsburgh, PA 15261

Mary Anne Alvin
National Energy Technology Laboratory
U.S. Department of Energy
Pittsburgh, PA 15236

ABSTRACT

An experimental study is performed to investigate the heat transfer characteristics and frictional losses in a rib roughened walls combined with detached pin-fins. The overall channel geometry (W=76.2 mm, E=25.4 mm) simulates an internal cooling passage of wide aspect ratio (3:1) in a gas turbine airfoil. With a given pin diameter, D=6.35 mm= ¼E, three different pin-fin height-to-diameter ratios, H/D = 4, 3, and 2, were examined. Each of these three cases corresponds to a specific pin array geometry of detachment spacing (C) between the pin-tip and one of the endwalls, i.e. C/D = 0, 1, 2, respectively. The rib height-to-channel height ratio is 0.0625. Two newly proposed cross-ribs, namely the broken ribs and full ribs are evaluated in this effort. The broken ribs are positioned in between two consecutive rows of pin-fins, while the full ribs are fully extended adjacent to the pin fins. The Reynolds number, based on the hydraulic diameter of the un-obstructed cross-section and the mean bulk velocity, ranges from 10,000 to 25,000. The experiment employs a hybrid technique based on transient liquid crystal imaging to obtain distributions of the local heat transfer coefficient over all of the participating surfaces, including the endwalls and all the pin elements. The presence of ribs has enhanced the local heat transfer coefficient on the endwall substantially by about 20% up to 50% as compared to the neighboring endwall. In addition, affected by the rib geometry, which is a relatively low profile as compared to the overall height of the channel, the pressure loss seems to be insensitive to the presence of the ribs. However, from the overall heat transfer enhancement standpoint, the baseline cases (without ribs) outperforms cases with broken ribs and full ribs.

NOMENCLATURE

A	Area
C	Detached spacing between pin-tip and endwall
D	Pin diameter, 6.35mm
D_h	Duct hydraulic diameter
E	Channel height
f	Friction factor, $(\Delta P/\rho U^2)(D_h/L)$
H	Pin height
H_r	Rib Height
h	Heat transfer coefficient
k	Thermal conductivity
L	Channel length
Nu	Nusselt number
P	Pressure
Pr	Prandtl number
Re	Reynolds number, UD_h/ν
S	Inter-pin spacing in longitudinal direction
T	Temperature
U	Bulk mean air velocity in a channel
W_r	Rib width
X	Inter-pin spacing in transverse direction

Greek Symbols

α	Thermal diffusivity
ρ	Density
ν	Viscosity

Subscript

o	Smooth channel
p	Pin
r	Row
T	Total or entire array
w	Endwall

INTRODUCTION

The gas turbine community continually seeks to increase the thermal efficiency and power output by increasing the turbine inlet temperature to beyond the melting temperature of turbine airfoil vanes and blades. Effective cooling schemes are required to protect the gas turbine components from failure. Many cooling techniques such as film cooling, pin fin cooling, and rib-turbulated cooling are employed to protect the airfoils, preventing the airfoils from failure while extending durability.

A pin-fin array is usually rows of short circular cylindrical elements generally arranged in staggered configurations in a narrow channel, with cooling fluid passing over the array. This appears to be an effective heat transfer enhancement method, but is accompanied with a pressure loss. These characteristics resemble the early studies of heat transfer over long tube bundles with cross flows for shell-and-tube heat exchangers. Pin fins are usually attached perpendicularly to both endwalls inside the narrow cooling channel of a gas turbine airfoil. Previous studies in pin-fin array heat transfer have been focused on the effects of array geometry and shape of the pin fins [1-12]. Amstrong and Winstanley conducted a review of pin-fin heat transfer and compiled the staggered-array data up to 1987 [1].

Van Fossen [2], Al Dabagh and Andrews [3] and Chyu et al. [4-7] reported that different flow characteristics in association with the heat transfer performances over the surfaces of pin fins and endwalls results in different levels of heat transfer on pin surfaces as well as on endwalls. Local and spatially-averaged heat transfer coefficients are reported for different pin-fin arrays, which reveal evidence of significant heat transfer augmentations for certain inline and staggered pin-fin arrays. For short pin fin arrays (e.g. H/D=1), also suggested in Chyu et al. [4] that array-averaged results are "virtually equal to the corresponding endwall averages," due partly to the fact that endwall often accounts for a significant portion of the total wetted area. Further detailed studies were reported by Won et al. [8] who investigated the spatially resolved heat transfer and flow structure in a rectangular channel with pin fins. They concluded that the local Nusselt numbers, measured on one of the symmetric endwalls, are highest beneath primary and secondary horseshoe vortices located immediately upstream to individual pins, beneath pin wakes, and downstream of the pin fins. These are regions where shear layers are positioned between the wakes behind the pins and the higher speed flow away from an individual pin. Using a hybrid measurement technique, Chyu et al. [5] investigated the effects of height-to-diameter ratio of pin fins on heat transfer for both pin fins and endwalls and reported that an increase in pin height leads to a higher overall heat transfer, but with a greater pressure loss. Park et al. [9] performed similar experiments using the naphthalene-sublimation technique to examine the rotation effects on the endwall heat transfer. While their overall averaged results show similar characteristics to previous data [5], the rotation effects induces notable difference in heat/mass transfer at the leading and trailing edge.

Near the trailing edge of an airfoil, pin fins are used not only for cooling purposes but also as part of mechanical structure to bridge the thin metallic pressure-surface and suction-surface. As a result, all pin elements are attached directly to both endwalls. However, this may not necessarily be the case for cooling the main body of a turbine airfoil. A recent study by Siw et al. [10] suggests that pin fins with a certain level of detachment from one of the endwalls can, in fact, promote more heat transfer than the corresponding cases with full endwall attachment. The sharp edge of pin tip detached from an endwall is expected to induce a higher level of turbulent mixing in the gas flow channel, thus further enhancing heat transfer and overall cooling effectiveness. The data reported by Siw et al. [10] indicate that an optimal heat transfer and pressure loss condition can be achieved when the gap between pin tip and endwall, C, is about one-quarter of the fully attached pin height, H; i.e. $C/H = ¼$. While the effects of detached gap have been limitedly studied in the pin fin literature, this finding is generally in agreement with previous studies in the open literature [11-13].

There exists a vast literature with respect to rib-turbulators studies conducted in both rotating and non-rotating channels that involve different combination of rib height, rib angle, rib spacing, rib shape, and inline or staggered rib configurations. Han et al. [14] compiled most of the findings related to rib-turbulators prior to year 2000. Earlier studies by Han et al. [15] using various rib configurations suggested that both 45^o parallel ribs and 45^o V-shaped ribs have similar performance and are better than those with 45^o crossed ribs, inverted V ribs and 90^o ribs. Later studies by Han et al. [16] further concluded that V-shaped broken ribs are better than the corresponding 60^o and 45^o parallel continuous ribs. Lee at al. [17] reported that V-shaped ribs in both stationary and rotating channel produce more heat transfer enhancement than the corresponding angled ribs.

Han and Park [18] studied the combined effects of rib angle and channel aspect ratio in rib-roughened rectangular channels and found that the heat transfer in the square channel with angled ribs is about 30% greater than that of the transverse rib case. Based on the experimental studies by Park et al. [19] with five channels of different aspect ratios and varying rib angles between 30^o and 90^o, their results concluded that a wide aspect ratio channel with rib angles of $45^o/30^o$ gives the best heat transfer enhancement. Apart from rib configurations, rib spacing and height in the internal cooling passages are important that have a certain impact on the heat transfer behavior. Placing too many ribs on the heat transfer surface could result in an increase in pressure drop. An insufficient number of ribs will result in minimal heat transfer due to minimal breaking of boundary layer. Taslim and Spring [20] used a liquid crystal technique to investigate the effects of rib profile, rib spacing, and blockage ratios on heat transfer and friction. Based on their experimental results, they reported the existence of an optimum pitch distance between neighboring ribs for any given blockage ratio.

Wright et al. [21] conducted experimental works with high aspect ratio channels that involve rotational effects. They reported that the discrete W-shaped and discrete V-shaped ribs have the greatest overall performance in comparsion to the standard angled ribs. Recently, Rallabandi et al. [22, 23] conducted experimental studies to explore the heat transfer and pressure loss in a stationary channel with square/sharp edged ribs for a wide range of Reynolds numbers ranging from 30,000 to 400,000. Their studies also included round edged ribs to take into account of manufacturing effects. The heat transfer performance is comparable for the round ribs and sharp ribs. The channel containing round ribs, however is more advantageous with slightly lower pressure drop due to less friction.

There exists extensive studies that are focused on either surface enhancement, such as vortex generators/turbulators, or turn effects, in exploring the characteristics of both heat transfer and pressure loss in cooling passages. Depending on different design and flow conditions, typical rib turbulators can promote an approximately 2.0 to 3.5 fold heat transfer enhancement, with a 6 to 10 times pressure loss, as compared to their smooth wall counterparts [24]. The turbine community and manufacturers are striving to improve the level of internal heat transfer enhancement to reduce the coolant consumption of external cooling. This will lead to an improved overall turbine efficiency.

The objective of this study is to investigate the combined effects of detached pin fins and rib roughness on the heat transfer and pressure characteristics in a cooling channel. To the authors' knowledge, there is no information of this nature reported in the open literature. Review of the literature suggests that V-shaped ribs induce a higher heat transfer enhancement than the angled ribs. Under this notion, two new v-shaped rib designs, one based on full ribs and other based on broken ribs, along with different gap sizes between pin-fin-tip and adjacent endwall have been investigated. With a given pin diameter, D=6.35 mm= ¼E, three different pin-fin height-to-diameter ratios, H/D = 4, 3, and 2, are examined. As the height of the test channel is kept the same, each of these three cases corresponds to a specific pin array geometry of detachment spacing (C) between the pin tip and the adjacent endwall, i.e. C/D = 0, 1, 2, respectively.

Test Section and Experimental Procedure

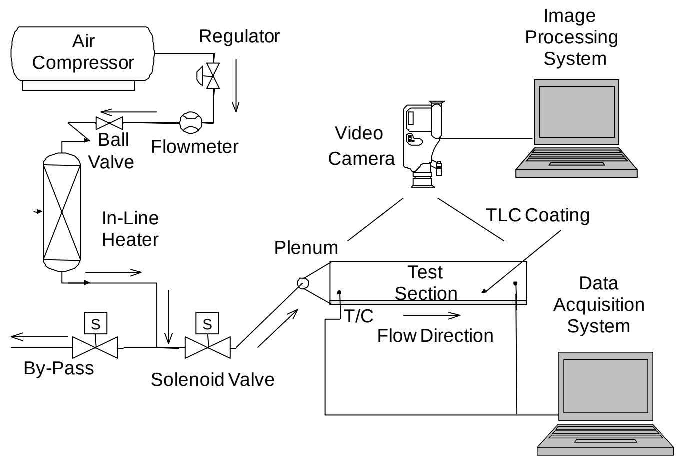

Fig. 1 Schematic Layout of the Test Setup

All heat transfer measurements in this study are conducted using a well documented transient thermochromic liquid crystal (TLC) technique [25-28]. The overall test setup is shown in Fig. 1. Compressed air, as the working fluid, is provided from an existing in-house air compressor and metered using an ASME orifice before entering the flow loop. Prior to the experiment, air is heated to a steady temperature (~60.0^{o}C ± 1.0^{o}C) using heaters connected in series to a variable transformer. Hot air is directed into the test section once the steady condition is reached. Images of the test domain were captured using a digital video camera mounted directly above the test section. Temperature of the air flow is measured throughout the test period using two thermocouples located at about 50mm upstream and downstream of the test section. These two thermocouple readings, representing the inlet and outlet temperatures across the test domain, are used to determine the bulk temperature profile in the test channel. The bulk temperature at any specific location along the test section is determined by linear interpolation between the measured inlet and outlet temperatures. These thermocouples are connected to a National Instruments SCXI 1000 Chassis via an NI SCXI 1303 terminal block. To characterize the pressure loss in the channel, pressure measurements are often done separately from the heat transfer tests, using pressure taps installed at the same locations as those of the thermocouples and an inclined manometer.

The test section shown in Fig. 1 is a rectangular channel of 76.2mm x 25.4mm (3.0" x 1.0"), made of 25.4mm thick Plexiglas. The low thermal conductivity of Plexiglas is necessary for the one-dimensional, semi-infinite heat transfer model on which the local heat transfer coefficient on the surface in between the adjacent pins is based. Pin fins are made from 6.35mm (1/4") diameter aluminum rods to ensure a very small Biot number so that each pin can be considered as a lump unit with uniform temperature. One end of the pin fins are threaded and screwed into the Plexiglas by 3.2mm (⅛"). Table 1 summarizes the test cases conducted in this study. The

Case	Pin-Fin Configurations	Pin Tip to Endwall Spacing Ratio, C/D	Pin-Fin Height to Pin Diameter Ratio, H/D on Top Endwall	Pin-Fin Height to Pin Diameter Ratio, H/D on Bottom Endwall
1	Staggered w/ Broken Ribs	1	3	3
2	Staggered w/ Broken Ribs	2	2	2
3	Staggered w/ Full Ribs	0	4	4
4	Staggered w/ Full Ribs	1	3	3
5	Staggered w/ Full Ribs	2	2	2

Tab. 1 Test Cases in This Study

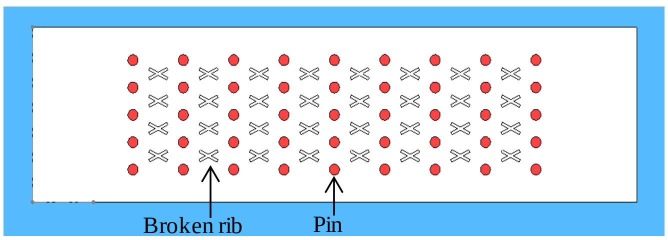

(a)

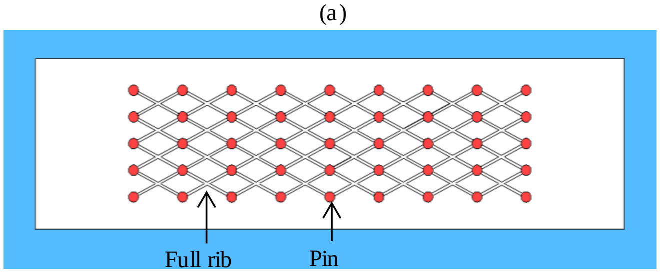

(b)

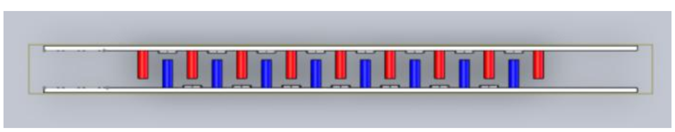

(c)

Fig. 2 Top View of (a) Broken Rib and (b) Full Rib Array (c) Staggered Pin-Fin Configuration (Side View)

pin-fin (D=6.35mm) arrays consist of staggered configurations, each with three different ratios of detached clearance to the pin diameter, C/D=0, 1 and 2. Since the height of the channel is 4 times the pin diameter, these cases correspond to a pin-height-to-diameter ratio of H/D=4, 3 and 2, respectively. Only the staggered array with both transverse pitch and longitudinal pitch equal to 2.5 times the pin diameter, i.e., S/D=X/D=2.5, is chosen for the study, as it is considered an optimal geometry for pin-fin induced heat transfer enhancement [10].

Figure 2 shows the schematic of pin-rib geometry viewed from the top and side of the channel. Both Fig. 2a and 2b show the top view of the top endwall mounted with pin-fins marked as 'red' color dots. Fig. 2c illustrates the side view of the staggered pin-fins configuration in the test section. 'Blue' color dots represent the pin fins mounted on the bottom (opposite) endwall. The top and bottom endwalls are identical and the bottom endwall is arranged by shifting one pitch (2.5D) downstream of the top endwall. All of the results presented in the following section are based on the data captured from the top endwall. All ribs have a square cross-section with 1.6mm (1/16") in width and height. Since the height of the channel is 25.4mm (1.0"), the rib-height-to-channel-height ratio is 1:16. Also, the ratio between the rib-height to pin-diameter is 1:4. For the broken rib cases (Fig. 2a), the length of the ribs is 12.7mm (0.5"), while for the full rib cases, the ribs are extended from one pin to another to the following row as shown in Fig. 2b.

The Reynolds number, based on the hydraulic diameter of the unobstructed cross-section (Dh) and bulk mean velocity (U) in the channel, as expressed below, ranges from 10,000 to 25,000.

$$\mathrm{Re} = \frac{\rho U D_h}{\mu} \qquad (1)$$

Results and Discussions

To resolve the heat transfer characteristics for both pin fins and the endwall, the current measurement approach is based on a hybrid technique which is a combination of two different but somewhat similar principles and well documented by Chen et al. [27]. Most of the results presented in this paper are in the form of a dimensionless heat transfer coefficient, the Nusselt number, Nu, which is defined as

$$Nu = \frac{hD_h}{k} \qquad (2)$$

The uncertainty analysis with a 95% confidence level on the Nusselt number ratio based on the method of Kline and McClintock [29] is about 8%. The uncertainty for pressure measurement is about 7%.

Local Heat Transfer Coefficient Distribution

Figure 3 and 4 show the results for the distribution of local heat transfer coefficient, h, for the endwall and pin fins with the additional effects from broken ribs and full ribs at Re=25,000. The results (staggered array with no ribs) from the most recent findings [10] are used as the baseline cases in comparison with the present study. The results are plotted according to the pin detached spacing, C/D=2 and C/D=1. Figure 3 and 4 show the same trend that the h values increase to a peak value at the third or fourth row, before decreasing towards a fully developed value.

Overall comparison of color contours in Fig. 3 and 4 clearly suggests that the broken rib case has the largest heat transfer coefficient among all cases. One plausible explanation that contributed to such phenomenon can be due to excessive vortices generated by the broken ribs while still preserving the

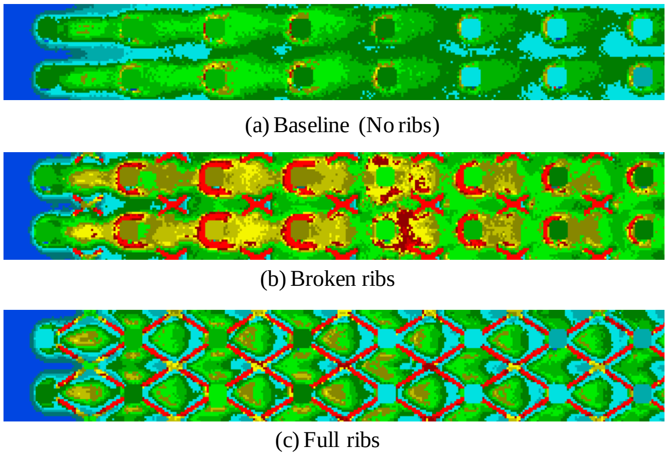

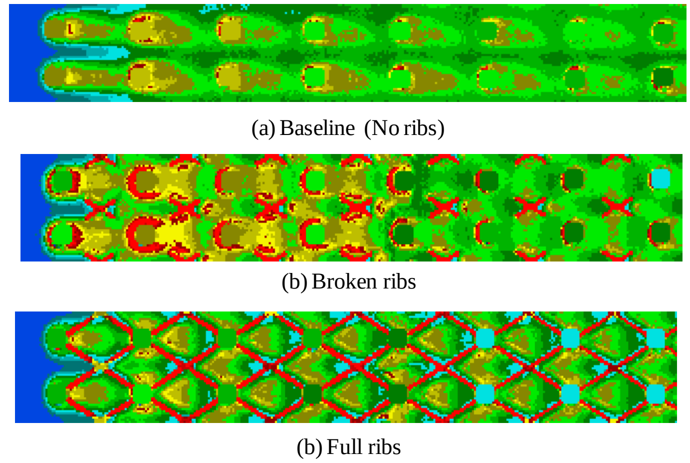

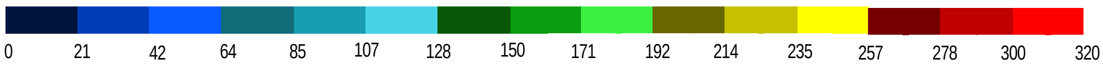

Fig. 3 Local Heat Transfer Coefficient, h (W/m2-K) Distribution for Endwall and Pin Fins (C/D=2; H/D=2) at Re=25,000

Fig. 4 Local Heat Transfer Coefficient, h (W/m2-K) Distribution for Endwall and Pin Fins (C/D=1; H/D=3) at Re=25,000

horseshoe vortices which are major contribution to heat transfer enhancement. Notably, the horseshoe vortices are largely preserved in the baseline and full rib cases. The significant advantage of having additional ribs is that the local heat transfer at the endwall is substantially enhanced as compared to the baseline cases. This is the main reason which explains that the h values on the endwall of both the broken rib and full rib cases surpassed the h values of the neighboring pin fins. This is a very substantial finding which contrasts with most literature [4-8] where the heat transfer from the pin fins is generally reported to be higher than that of the neighboring endwall.

In the full rib cases, heat transfer downstream of the ribs is low due to relatively hot cell being trapped as a result of recirculation. However, when the mainstream gas reattaches (between two consecutive rows), the heat transfer is increased due to impingement from the mainstream gas on the surface. The presence of broken ribs has only significant effects on the local heat transfer surrounding the ribs. Similar heat transfer patterns due to separation and reattachment are not observed in the broken rib cases.

In all baseline cases, the heat transfer on the pin fins is higher than the neighboring endwall. This trend is reversed after the fifth row. A slight difference is observed in the broken rib and full rib cases where the heat transfer pattern between the pin fins and endwall has a reverse trend as compared to the baseline cases. Throughout the entire domain, the endwall has a larger heat transfer in comparison to the neighboring pin fins except for the first row. The data shows that decreasing the detached pin space from C/D=2 to C/D=1, contributed to an overall enhancement of about 10% in overall heat transfer results.

Row-Resolved, Average Nusselt Number

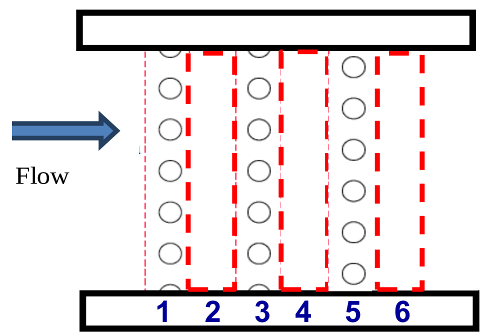

Fig. 5 Schematic of Row in the Pin-Fin Array

The results in this section present the row-resolved averaged Nusselt number of the pin fins and endwall for the cases shown in Table 1, with Re ranging from 10,000 to 25,000. The captions “S”, “FR”, “BR”, “w”, and “p” in these figures stand for “staggered array as baseline”, “full ribs”, “broken ribs”, “endwall” and “pin fins”, respectively. The captions “2”, “3”, and “4” denote the height of the pin fins normalized by the pin diameter, (i.e., 2 represents pin fins H/D=2, C/D=2). The domain of a given row is centered at the location of the pin axis and extends one-half of the longitudinal spacing both upstream and downstream as shown in Fig. 5.

Figure 6 and 7 illustrates the row-resolved averaged Nusselt number for endwall and pin fins of the broken rib and full rib cases with pin fins H/D=2 (i.e., C/D=2) and H/D=3 (i.e., C/D=1) in comparison to the baseline cases (staggered array without ribs). The results in Fig. 6 show that the magnitude of heat transfer increment on the endwall with Re

Endwall **Pin Fins**

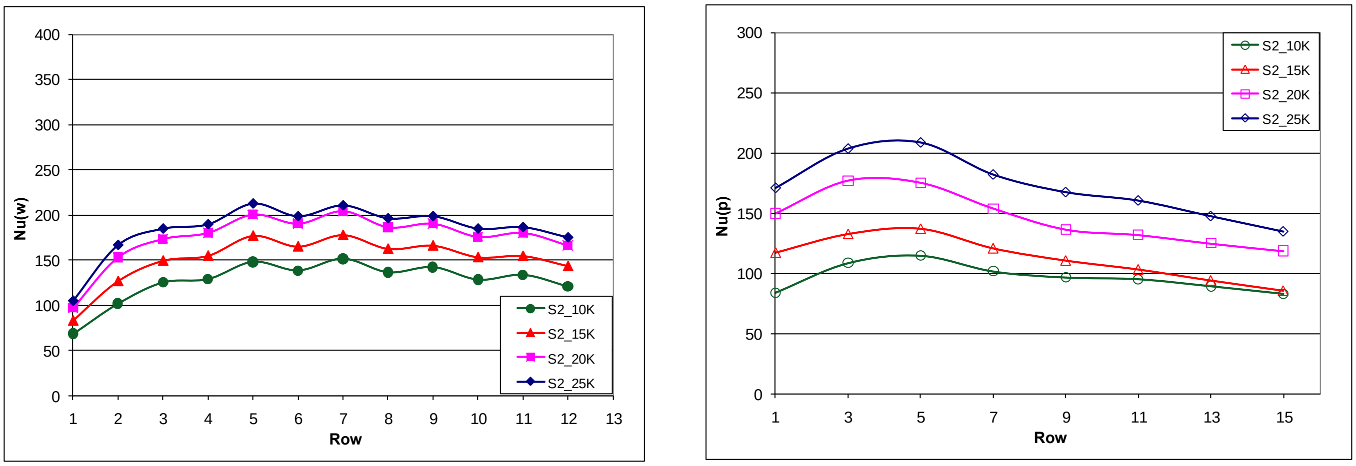

(a) Baseline, Pin Fins (C/D=2; H/D=2) No Ribs

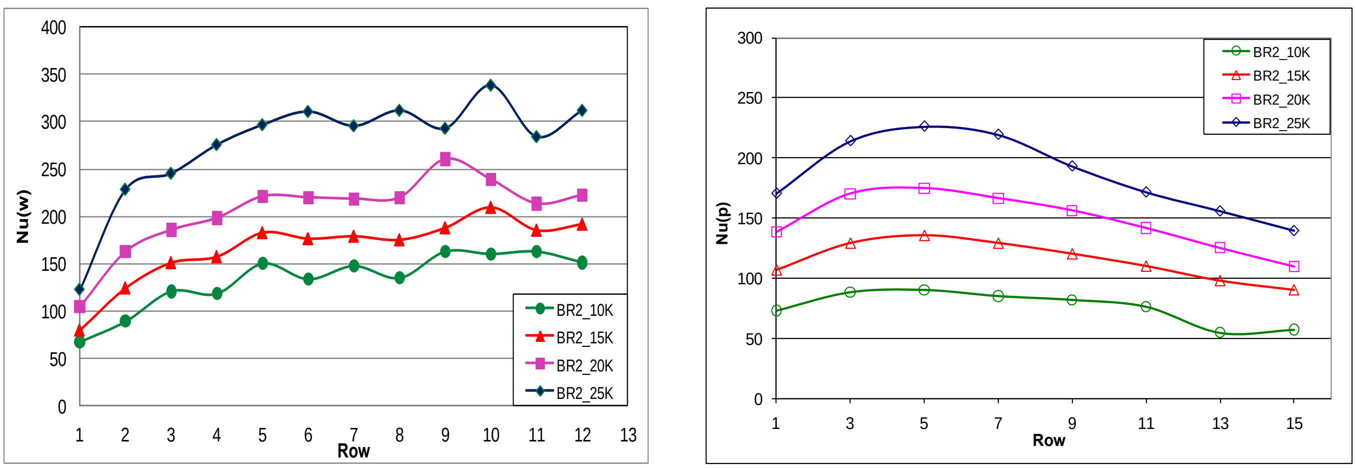

(b) Pin Fins (C/D=2; H/D=2) with Broken Ribs

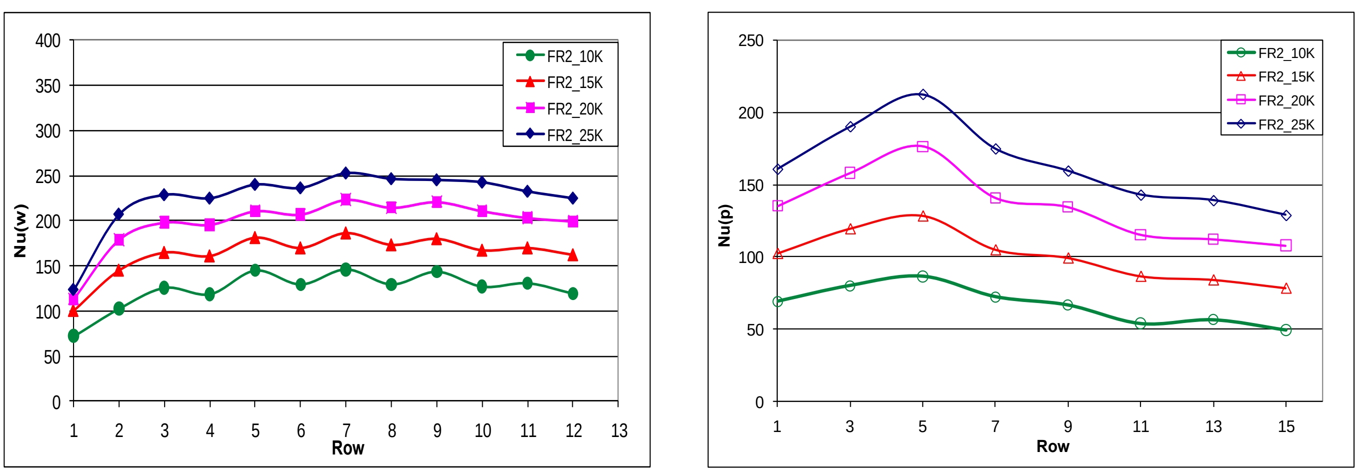

(c) Pin Fins (C/D=2; H/D=2) with Full Ribs

Fig. 6 Row-Resolved Average Nusselt Number for Endwall and Pin Fins (C/D=2; H/D=2) (a) Baseline (b) Pin Fins with Broken Ribs (c) Pin Fins with Full Ribs

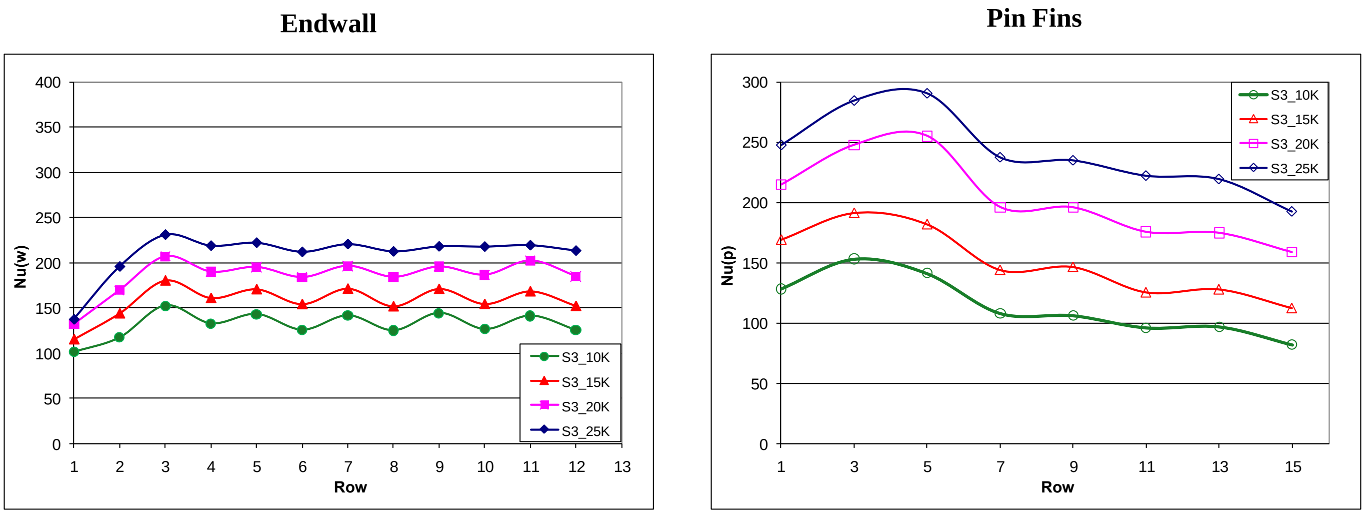

(a) Baseline, Pin Fins (C/D=1; H/D=3) No Ribs

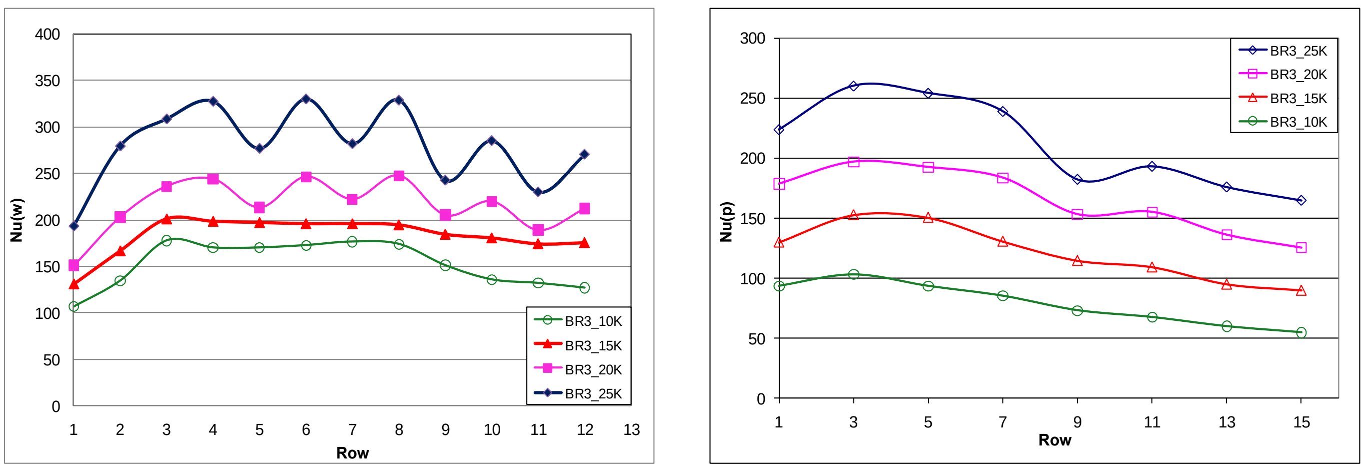

(b) Pin Fins (C/D=1; H/D=3) with Broken Ribs

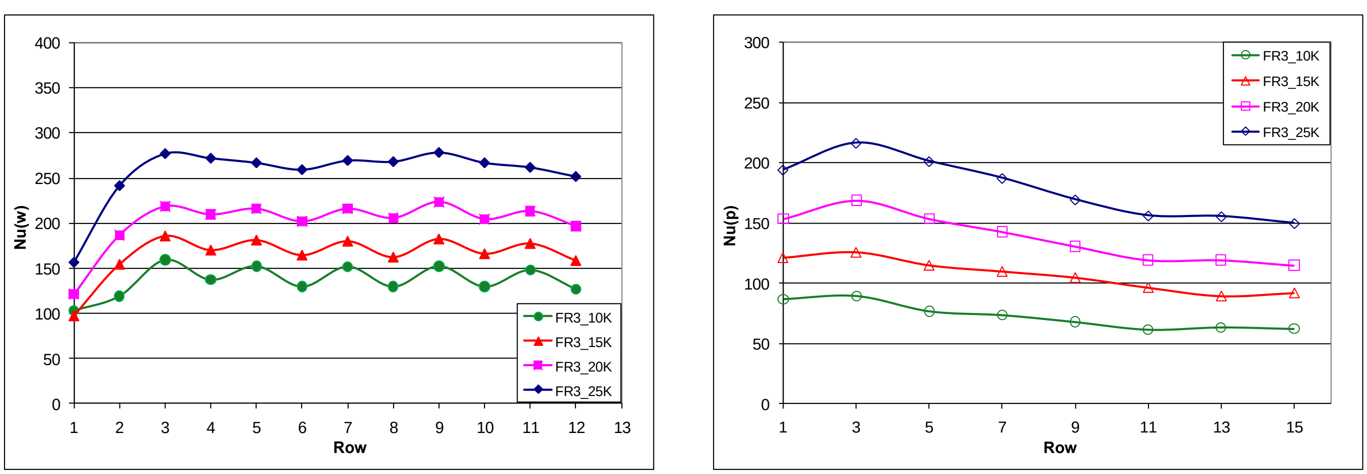

(c) Pin Fins (C/D=1; H/D=3) with Full Ribs

Fig. 7 Row-Resolved Average Nusselt Number for Endwall and Pin Fins (C/D=1; H/D=3) (a) Baseline (b) Pin Fins with Broken Ribs (c) Pin Fins with Full Ribs for the baseline case is the lowest compared to the broken and full rib cases. This is more evident in the broken rib case as the Re increases. Generally, heat transfer on the endwall alone for the broken rib and full rib cases are higher than the baseline cases by about 10% to 25%. However, at the lowest Re (i.e., Re=10,000), the heat transfer on the endwall for all cases is comparable. Heat transfer from pin fins in all cases at Re=10,000 are also relatively close, which suggests that the bulk flow fields in the core region behave similarly. However, with the presence of ribs, heat transfer on the ribs and the neighboring region is enhanced significantly. Overall, the heat transfer on the endwall exceeds that on the pin fins by 10% up to 50%.

Based on Fig. 7, the magnitude of heat transfer on the endwall is higher than that of the cases with shorter pin fins (i.e., H/D=2; C/D=2), with the exception for the broken rib case. This is predictable as the flow experiences greater disturbances due to more obstructions from the longer pin fins. For the broken rib cases, at higher Re, i.e., Re=20,000 and 25,000, heat transfer increases drastically and varies over a larger scale throughout the entire domain. Heat transfer on the endwall is higher than that of the neighboring pin fins for the broken rib and full rib cases, by about 10% to 25%.

For the baseline cases, the results in both Fig. 6 and 7 show an opposite heat transfer pattern between the pin fins and neighboring endwall as compared to the ribs cases. Heat transfer from pin fins is higher than that of the neighboring endwall by 10% up to about 20%. Evidently, this shows that the separated shear layers generated by the pin tip alone and the pin-to-endwall interaction have a more dominating impact on pin fin heat transfer than the combination of detached pin space and ribs. Such effects decrease as the flow progresses towards downstream, and eventually heat transfer on the endwall becomes greater than that of the pin fins.

Overall Averaged Heat Transfer Coefficient

Figure 8 and 9 reveals the heat transfer enhancement of the full ribs and broken ribs cases normalized by the fully developed smooth channel in comparison with the baseline cases. The value of Nu_o is based on the Dittus-Boelter correlation:

$$Nu_o = 0.023\, Re^{0.8}\, Pr^{0.4} \qquad (3)$$

The magnitude of Nu_w is calculated based on heat transfer coefficient contributed by the endwall only and weighted by the wetted area, i.e.,

$$Nu_w = \frac{\sum Nu_w \times A_w}{\sum A_w} \qquad (4)$$

while the magnitude of Nu_T is calculated by combining the heat transfer coefficient contributed by both the pin-fins and the endwall and weighted by the size of the wetted area, i.e.,

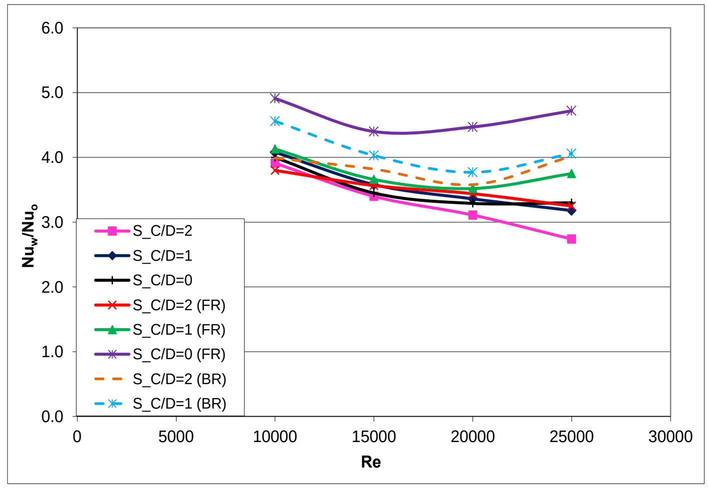

Fig. 8 Endwall Heat Transfer Enhancement vs Re

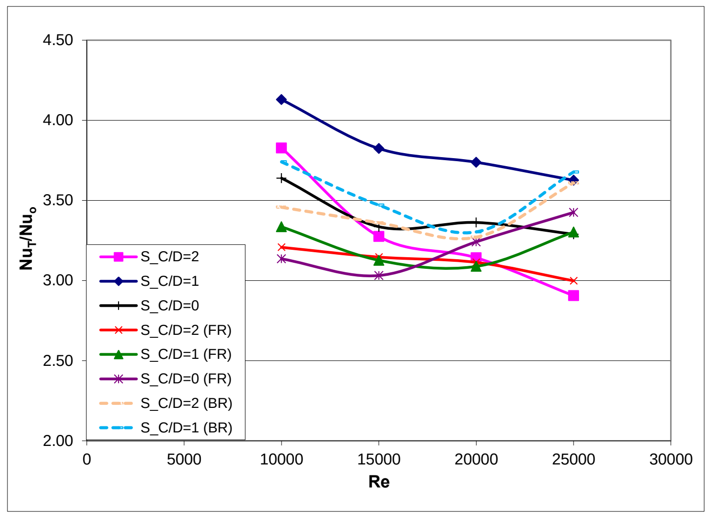

Fig. 9 Overall Heat Transfer Enhancement vs Re

$$Nu_T = \frac{\sum Nu_p \times A_p + \sum Nu_w \times A_w}{\sum A_p + \sum A_w} \qquad (5)$$

The results in Fig. 8 reflect the local trend and row-resolved average Nusselt number delineated earlier. Full ribs are very effective in enhancing heat transfer when coupled with fully bridged pin fins. This is clearly shown in Fig. 8 as the full rib case with fully bridged pin fins exhibits the highest heat transfer factor ranging from 4.3-4.9. The broken rib cases of C/D=1 and C/D=2 show rather high heat transfer factor as well that range from 3.6-4.5. The baseline case of C/D=2 has the lowest heat transfer factor. For the same detached pin-fins height, all broken rib cases outperform the full rib cases by about 10-15%. Generally, the results indicate that both broken and full rib cases outperform the baseline cases.

While previous results show that both broken rib and full rib cases have significant impact towards the heat transfer on the endwalls. However, by considering the magnitude of heat transfer and overall effective heat transfer area in the domain, the result in Fig. 9 clearly indicates that ribs have adverse effects on the overall heat transfer in the entire channel. The baseline case, C/D=1 remains the best performer among all. Therefore, this concludes that ribs significantly affect the endwall heat transfer, while heat transfer on pin fins is solely enhanced due to the detachment effect alone. Among the full rib cases, the case of with the shortest pin fins, C/D=2 has the worst heat transfer enhancement. Other full rib cases, C/D=1 and C/D=0, exhibits comparable heat transfer enhancement but about 10-15% lower as compared to the baseline counterpart. The broken rib cases outperform the full rib cases by about 10%, but still underperform as compared to the baseline case, C/D=1. However, at high Re, the level of heat transfer enhancement in the broken rib cases seems to increase and comparable to the baseline case, C/D=1.

The result in Fig. 9 also illustrates that all baseline cases (without ribs) have better heat transfer enhancement than the full rib and broken rib cases by about 5%-10% except for the cases with pin fins C/D=2. For the case with the largest pin detached space, C/D=2, presence of broken ribs is favorable as the results show that overall heat transfer enhancement has increased by about 5% as compared to the baseline case.

Pressure Loss Coefficient

Heat transfer enhancement is usually accompanied by the penalty of additional pressure loss. Any element protruding from the endwall (i.e., pin fins and ribs), will obstructs the flow causing drag and head loss in the system. The pressure loss characteristics of all cases presented in Fig. 10 are based on f/f_o, where f is the friction factor, defined by:

$$f = \frac{2D_h}{\rho U^2}\left|\frac{dP}{dx}\right| \tag{6}$$

and f_o is the overall friction factor normalized by the corresponding data for fully developed flow in a smooth channel developed by Petukhov:

$$f_o = (0.790 \ln Re - 1.64)^{-2} \quad 3000 \le Re \le 5\times10^6 \tag{7}$$

The parameter dP/dx represents the pressure drop across the test section by measuring the streamwise static pressure distributions upstream and downstream of the test section. Most cases seem to have fairly constant pressure loss with respect to Re and the result shows that the pressure drop increases with pin fins height. As the height of the ribs is 1/16" (1.6mm) which is about 6% of the channel height, the presence of broken ribs and full ribs imposed insignificant pressure loss to the entire domain as compared to the baseline cases. Pressure drop in both broken rib and full rib cases is about 5%-8% higher than the baseline cases.

Performance Index

The assessment of performance for a pin-fin array is measured by the performance index, PI, defined as

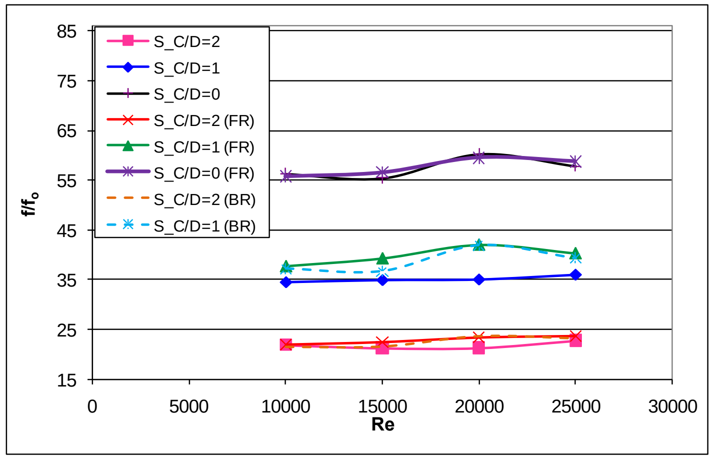

Fig. 10 Pressure Loss Coefficient vs Re

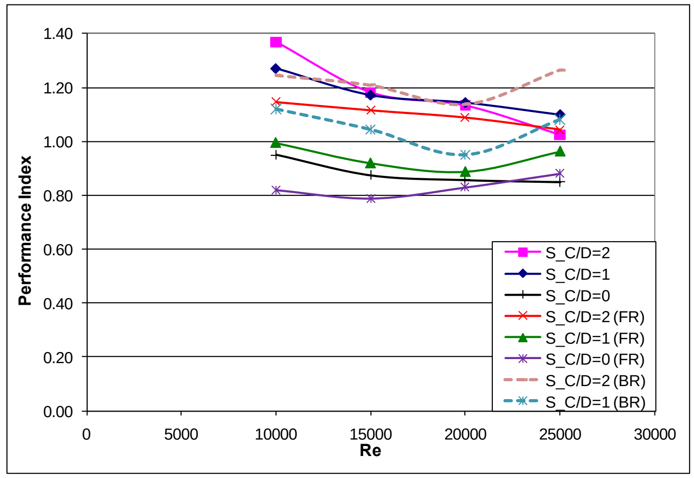

Fig. 11 Performance Index vs Re

$$PI = \frac{Nu_T / Nu_o}{(f/f_o)^{1/3}} \tag{8}$$

Fig. 11 illustrates the performance index for all cases in comparison to the baseline results from previous section. With low heat transfer enhancement, but coupled with relatively low pressure loss, broken ribs with pin detached space of C/D=2 yields the highest PI together with baseline case C/D=1 and C/D=2. For all fully bridged pin-fins cases, C/D=0 which has moderate heat transfer enhancement and is penalized with the largest pressure loss, has the lowest PI. At the same pin detached space, C/D=2, the full rib case has slightly lower PI (i.e., by about 5%) as compared to the broken rib case. All broken rib cases outperform the full rib cases with pin-fins C/D=1 and 0 by about 10% -20%.

Conclusions

The present study performs a systematic investigation with respect to the effects of detached spacing of pin-fin arrays on the heat transfer in a rib-roughened channel. The geometry and test conditions are relevant to advanced cooling concepts with three-dimensional protruding elements, combined with two-dimensional elements, for enhancement of turbine airfoil internal cooling. The concept of implementing pin fins with detached spacing between the pin tip in the rib roughened channel is to promote turbulent convection with separated shear layers induced near the pin tips together with separation and reattachment effects from the ribs that could further enhanced the overall heat transfer.

The presence of broken ribs and full ribs has significant effects on endwall heat transfer enhancement only. Broken ribs and full ribs are effective in enhancing the heat transfer on the endwall only by gaining an additional 10%-20% as compared to the baseline cases. Fully bridged pin fins with full rib case provide the highest heat transfer factor on the endwall, ranging from 4.3-4.9. Ribs, however, posed an adverse effect on the test domain. The presence of ribs which alter the horseshoe vortices has reduce the heat transfer on the pin fins by about 10% to 50% as compared to the neighboring endwall. From the overall heat transfer enhancement standpoint, the baseline case of C/D=1 remains as the best choice among all cases currently explored. As the height of the ribs constitutes about 6% of the channel height, the presence of ribs imposed insignificant pressure loss as compared to the baseline cases. Based on the PI, the baseline case of C/D=1 remain as the best choice among all cases together with C/D=2 baseline and broken rib cases. Overall comparison in terms of PI shows that broken rib cases outperform the full rib cases by 10% to 20%.

Acknowledgement

This research effort was performed in support of the National Energy Technology Laboratory under Contract DE-FE-0004000. The authors wish to thank Mr. Richard Dennis at DOE NETL for his continued support.

References

1. Armstrong, J., and Winstanley, D., 1988, "A Review of Staggered Array Pin Fin Heat Transfer for Turbine Cooling Applications," ASME J. Turbomach., 110, pp. 94-103.
2. VanFossen, G.J., 1982, "Heat Transfer Coefficients for Staggered Arrays of Short Pin Fins," ASME J. Eng. Power, 104, pp. 268-274.
3. Al Dabagh, A. M., and Andrews, G.E., 1992, "Pin-Fin Heat Transfer: Contribution of the Wall and the Pin to the Overall Heat Transfer," ASME Paper 92-GT-242.
4. Chyu, M.K., Hsing, Y.C., Shih, T.I.-P., and Natarajan, V., 1999, "Heat Transfer Contributions of Pins and Endwall in Pin-Fin Array: Effects of Thermal Boundary Condition Modeling," ASME J. Turbomach., 121, pp. 257-263.
5. Chyu, M.K., Siw, S. and Moon, H.K., 2009, "Effects of Height-to-Diameter Ratio of Pin Element on Heat Transfer from Staggered Pin-Fin Arrays," GT2009-59814, ASME Turbo Expo 2009, Orlando, June 8-12, 2009.
6. Chyu, M.K., and Goldstein, R.J., 1991, "Influence of an Array of Wall-Mounted Cylinders on the Mass Transfer from a Flat Surface," Int. J. Heat Mass Transfer, 34(9), pp. 2175-2186.
7. Chyu, M.K., 1990, "Heat Transfer and Pressure Drop for Short Pin-Fin Arrays and Pin-Endwall Fillet," ASME Trans.-J. Heat Transfer, 112 (4), pp. 926-932.
8. Won, S.Y., Mahmood, G.I., and Ligrani, P.M., 2004, "Spatially-Resolved Heat Transfer and Flow Structure in a Rectangular Channel with Pin Fins," Int. J. of Heat and Mass Transfer, 47, pp. 1731-1743.
9. Park, J.S., Kim, K.M., Lee, D.H., Cho, H.H., and Chyu, M.K., 2008, "Heat Transfer on Rotating Channel With Various Height of Pin Fins," ASME Turbo Expo, GT2008-50783.
10. Siw, S.C, Chyu, M.K. and Alvin, M.A., 2010, "Effects of Pin Detached Space on Heat Transfer and Pin-Fin Arrays", ASME Paper No. GT2010-23227.
11. Steuber, G.D., and Metzger, D.E., 1986, "Heat Transfer and Pressure Loss Performance for Families of Partial Length Pin Fin Arrays in High Aspect Ratio RectangularDucts," 8th International Heat Transfer Conference, Vol 6, pp. 2915-2920.
12. Arora, S.C. and Abdel-Messeh, W., 1989, "Characteristics of Partial Length Circular Pin Fins as Heat Transfer Augmentators for Airfoil Internal Cooling Passages," ASME Paper 89-GT-87.
13. Chang, S.W., Yang, T.L., Huang C.C., and Chiang, K.F., 2008, "Endwall Heat Transfer and Pressure Drop in Rectangular Channels with Attached and Detached Circular Pin–Fin Array," Int. Journal of Heat and Mass Transfer, 51, pp. 5247-5259.
14. Han, J.C., Dutta, S., and Ekkad, S.V., 2000, "Gas Turbine Heat Transfer and Cooling Technology," Taylor and Francis.
15. Han, J.C., Zhang, Y.M., and Lee, C.P., 1991, "Augmented Heat Transfer in Square Channels with Parellel, Crossed, and V-Shaped Angled Ribs," ASME J. of Heat Transfer, Vol. 113, pp. 590-596.
16. Han, J.C., and Zhang, Y.M., 1992, "High Performance Heat Transfer Ducts with Parellel Broken and V-Shaped Broken Ribs," Int. J. of Heat and Mass Transfer, Vol. 35, No. 2,pp. 513-523.
17. Lee, E., Wright, L.M., and Han, J.C., 2003, "Heat Transfer in Rotating Rectangular Channels (AR=4:1) with V-Shaped and Angled Rib Turbulators with and without Gaps," ASME Paper No. GT2003-38900.
18. Han, J.C. and Park, J.S. 1988, "Developing Heat Transfer in Rectangular Channels with Rib-Turbulators," Int. J. of Heat Mass Transfer, Vol. 31, pp. 183-195.
19. Park, J.S., Han, J.C., and Huang, Y., Ou, S., 1992, "Heat Transfer Performance Comparisons of Five

Different Rectangular Channels with Parellel Angled Ribs", Int. J. of Heat Mass Transfer, Vol. 35, No. 11, pp. 2891-2903.
20. Taslim, M.E., and Spring, S.D., 1994, "Effects of Turbulators Profile and Spacing on Heat Transfer and Friction in a Channel," J Thermophysics Heat Transfer, Vol. 8, pp. 555-562.
21. Wright, L.M., Fu, W.L., and Han, J.C., 2004, "Thermal Performance of Angled, V-Shaped, and W-Shaped Rib-Turbulators in Rotating Rectangular Cooling Channels (AR4:1)," ASME Paper GT2004-54073.
22. Rallabandi, A.P., Yang, H., and Han J.C., 2009 , "Heat Transfer and Pressure Drop Correlations for Square Channels with 45 Deg Ribs at High Reynolds Numbers", J. Heat Transfer, Vol. 131, 071703-1-10.
23. Rallabandi, A.P., Nawaf, A., and Han J.C., 2009 , "Heat Transfer and Pressure Drop Measurements for Square Channels with 45 Deg Round Edged Ribs at High Reynolds Numbers", ASME Paper No. GT2009-59546.
24. Chyu, M.K., "Recent Advances in Turbine Heat Transfer-with A View of Transition to Coal Gas Based Systems," International Heat Transfer Conference, IHTC-14.
25. Metzger, D.E. and Larson, D.E., 1986, "Use of Melting Point Surface Coatings for Local Convection Heat Transfer Measurements in Rectangular Channel Flows with 90-Deg Turns," J. Heat Transfer, 109, pp 48-54.
26. Chyu, M.K. Ding, H., Downs, J.P. and Soechting, F.O., 1998, "Determination of Local Heat Transfer Coefficient Based on Bulk Mean Temperature Using a Transient Liquid Crystal Technique," J. Experimental Thermal and Fluid Science, 18, pp. 142-149.
27. Chen, S.P., Li, P.W., and Chyu, M.K., 2006, "Heat Transfer in a Airfoil Trailing Edge Configuration with Shaped Pedestals Mounted Internal Cooling Channel and Pressure Side Cutback," ASME Turbo Expo, GT2006-91019.
28. Chyu, M.K., Oluyede, E.O., and Moon, H-K., 2007, "Heat Transfer on Convective Surfaces with Pin-Fins Mounted in Inclined Angles," ASME Turbo Expo, GT2007-28138.
29. Kline, S.J. and McClintock, F.A., "Describing Uncertainties in Single Sample Experiments," Eng. (Am. Soc. Mech. Eng.), 75, pp. 3-8.